

**ON THE EFFECT OF THE SPATIAL VARIABILITY ON THE THM
BEHAVIOUR OF TUFFEAU STONE OF HISTORICAL BUILDINGS**

Naima Belayachi¹, Dashnor Hoxha¹ and Laura Michel¹

¹*Laboratoire PRISME, (EA4229) Polytech'Orléans, rue Léonard de Vinci, 45072
Orléans cedex 2, France*

Abstract

The cyclic stress fluctuation and fatigue due to everyday fluctuation of temperature and humidity is pointed out to be a crucial mechanism on deterioration of historical building. This paper deals with the role of stone properties variability on the amplification of stress variation and fatigue. Thus, the randomness and spatial variability of the mechanical, thermal and hydraulic properties are taken into account in a finite elements model of typical stone wall masonry of Chambord Castle. A methodology to examine the fatigue weathering of stone historical building due to climatic conditions and the heterogeneities of the stone properties the stress distribution of masonry structures integrating geostatistical analysis is presented.

Keywords: finite elements, masonry structures, stress distribution, spatial variability, variomap

1. Introduction

The knowledge of the structure, materials and their characteristics, the state of damage is essential for studying and modeling the behaviour of historical buildings in order to understand the weathering factors of stones. Salt weathering (salt crystallization in pores) (Rodriguez-Navaro 1999), atmosphere pollution, wetting and drying, severe frost or heating are known like the principal processes acting to weaken and deteriorate the stone (Nicholson 2000). A large number of experimental works were dedicated to reproduce the in-situ environmental conditions in order to identify causes and combined effects for weathering mechanisms (Beck 2006) (Castellanza 2004).

In the framework of SACRE research program one of the objectives was the quantification of the role of the daily meteorological conditions in the weathering of tuffeau stone buildings. The tuffeau is a porous limestone used in so-known Chateaux de la Loire castles in the Center region (France). Consequently, the thermo-hydro-mechanical analysis for unsaturated porous media was used to study the behaviour of stone wall. These studies have shown the role of daily variation of temperature and humidity on the damage of the stone (Belayachi 2012). However in these studies a deterministic approach has been used which does not explain the nonuniformity of deterioration faces and rates. These difference on deterioration from one point to another of the same building are not only due to differences of microenvironmental conditions but also to natural heterogeneity and the spatial variability of the physical, chemical and mechanical properties of stone block (Warke 2006). Several factors can be at the origin of this variability like mineralogical composition, porous microstructure and random grains arrangement (Moropoulou 2006).

Following above mentioned works on thermo-hydro-mechanical modeling of stone wall behaviour in this paper the effort is focused on the influence of the spatial variability of stone properties on the stress fluctuations. For that the same mathematical and physical framework is used for modeling but some key properties are supposed to be random quantities. The obtained results are then treated by geostatistical tools in order to shed light on the role of heterogeneous nature of the tuffeau stone as a potentially mechanism on the damage and deterioration

2. Outlines of numerical modelling

This research proposes a numerical approach to evaluate the effect of the heterogeneous nature of the stone on the deterioration processes. For that, the modelling is composed of two main parts. The first one allows the prediction of the behaviour of stone structure and the assessment of various quantities. The second part is inspired from the geostatistic variography analysis (Iwashita 2005), generates the stress distributions. The geometrical model chosen in the study is a wall stone masonry with mortar joint because of this is the construction type used in Chambord Castle and the majority of stone building. At the highlight of certain works (Chau 2006) the numerical models and tools developed for geomaterials are used (Chavant 2009) for stones considered as soft rocks. However, tuffeau stone and mortar are considered as an unsaturated porous material with solid phase, liquid phase (water) and gaseous one (dries air and water vapor) contained in pores system. Thus, the thermo-hydro-mechanical coupling model is based on the theory of mechanics of porous media (Coussy 2004) and the finite element code ASTER (Chavant 2009).

2.1 Thermo-hydro-mechanical model

We present in this section the essential of equations for coupled thermo-hydro-mechanical model, details are given in (Coussy 2004).

The well-known effective stress taking into account the effect of temperature and relative humidity is done:

$$\underline{\underline{\sigma'}} = \underline{\underline{\sigma}} + b\pi\underline{\underline{\delta}} + 3\alpha K\underline{\underline{\Delta T}}\underline{\underline{\delta}} \quad [1]$$

Where the second and third terms in Eq. 1 present coupling terms respectively for hydro mechanical and thermo mechanical behaviour respectively through Biot's coefficient ($b = 1 - K/K_s$) and thermal expansion coefficient α . The parameters K and K_s are bulk modulus of the drained medium and solid grains, respectively. In the case of saturated media, π represent interstitial pressure but for the unsaturated media it is a function of liquid saturation S_{lq} and capillary pressure P_c (difference of the gaseous and liquid pressure $P_c = P_g - P_l$) (Coussy 2004):

$$\pi = \begin{cases} \int_{S_{lq}}^1 S_{lq}(P_c) dP_c & \text{if } S_{lq} < 1 \\ P_l & \text{if } S_{lq} > 1 \end{cases} \quad [2]$$

The function $S_{lq}(P_C)$ represents the isothermal sorption curve of the material, which must be evaluated by experimental tests. In this study and for numerical considerations the tuffeau sorption curve that has been previously investigated experimentally (Beck 2006) can be approximated by an empirical Van Genuchten expression:

$$S_{lq}(P_C) = \left[1 + \left(\frac{P_C}{P_r} \right)^n \right]^{\frac{1-n}{n}} \quad [3]$$

Where P_r (stress units) and n (dimensionless) are two fitting parameters. The capillary pressure P_C can be evaluated from the relative humidity by considering the perfect gases law (Kelvin's law):

$$P_C = \frac{\rho_l \cdot R \cdot T}{M_l^{ol}} \ln(Hr) \quad [4]$$

where R , M_l^{ol} are, respectively, the constant of perfect gases the molar mass of water and Hr is relative humidity.

The flow of gaseous and liquid phase is governed by generalized Darcy's law:

$$\frac{M_j}{\rho_j} = -\lambda_j \underline{grad}(P_j) \quad j = \text{liquid, gas} \quad [5]$$

Where the flux vector M_j is proportional to the effective hydraulic conductivity l_j in unsaturated media of each phase (liquid, gas). This hydraulic conductivity is defined as:

$$\lambda_j = \frac{k_{in} \cdot k_j^{rel}(S_l)}{\mu_j} \quad j = \text{liquid, gas} \quad [6]$$

where k_{in} is the intrinsic permeability and k_j^{rel} the relative permeability, a limited value function of liquid saturation S_{lq} taking values between 0 and 1.

The relative movement of the vapour in the mixture of gases (air and vapour) is described by Fick's laws diffusion:

$$\frac{M_v}{\rho_v} = -F \underline{grad}(C_{vp}) \quad [7]$$

C_{vp} and F are respectively concentration of vapor in gaseous phase and Fick's coefficient. This equation can be rewritten as follow by considering of the uniform pressure of gases:

$$\frac{M_v}{\rho_v} = -\frac{F}{P_g} \underline{\text{grad}P_v} \quad \text{with } P_v \text{ being the vapor pressure} \quad [8]$$

To complete the transfer equations, the heat transfer is governed by Fourier's law:

$$\underline{q} = -\lambda_T \underline{\text{grad}(\Gamma)} \quad [9]$$

with \underline{q} being the thermal flux and λ_T thermal conductivity.

In this study, the proposed modeling consists in combining the heterogeneous stone nature and variation of climatic conditions to evaluate the effective stresses. So a linear elastic model is considered to describe the behaviour of both tuffeau stone and mortar to avoid other non linear mechanisms.

2.2 Spatial variability of stone properties

We present in this section the methodology used to describe spatially heterogeneous damage zones in stone block by geostatistical approach. This analysis was pioneered in mining, petroleum engineering and hydrogeology because it permits a statistical or probabilistic description of the spatial variability of the properties, which is inherent in both natural and artificial geomaterials. For example the influence of heterogeneous fault zones on permeability, fluid flow, chemical changes and their interactions in rock massifs has been recognized by several authors (Lopez 1996, Schulz 2000). The fundamental tool of the geostatistics is the variogram that is a variability measure related to distance based on the variance at two different locations (Yupeng 2011). Usually, the variogram estimation is calculated from the sampled experimental data set. In this study, the estimation of the stress variance is carried out between the results of the simulation with homogeneous stone and heterogeneous stone at each node of the stone block. As for the variomaps, they are carried out by the directional variogram obtained from the results on mesh grids of stone block. Therefore, we attempt to explain initially the geometrical model of the masonry structure, the boundary conditions before the simulation with the spatial variability.

In this macro-modelling the stone structure is treated as an equivalent continuum with average properties of stone blocks and mortars (Belayachi 2012) except on a part of wall where a stone block is explicitly modelled between two joints of mortar (Figure 1) in order to examine the differences of the properties in the generation of stresses. The tuffeau stone wall is modelled in plane strain configuration by a vertical cut perpendicular to the stretch of the wall. The thickness of this cut is of 80 cm and the high is 15 m corresponding to historical Castle walls. A perfect adherent interface is assumed between the stone block and mortar. The initial temperature and relative humidity are considered uniform in the wall and equal to $T_0=20^\circ\text{C}$ and $RH_0=53\%$ respectively. The effect of initial state has been studied in previous investigation (Belayachi 2012).

The Figure 1 shows the boundary conditions on the outdoor surface (right boundary), the indoor one (left boundary) and the finite element mesh. The temperature and relative humidity applied on the outdoor surface are obtained by a statistical analysis of time series en meteorological data around Chambord castle.

The thermo-hydro-mechanical description identifies several material parameters. For the tuffeau stone and joint mortar of Chambord castle, in previous experimental investigation the material properties are available (Beck 2006). Some of mortar parameters like the thermal expansion coefficient and isothermal sorption curve are identified by an inverse analysis based on the in-situ measured data. The relative liquid permeability is chosen as a third power function.

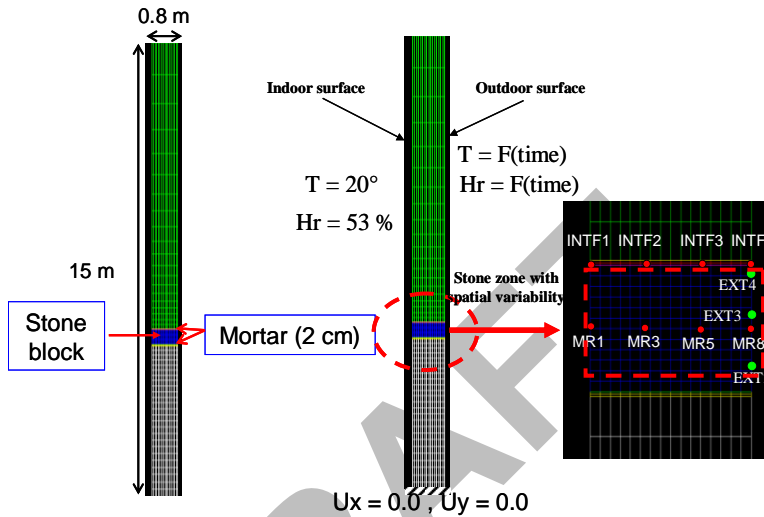


Figure 1. Geometrical finite element model and boundary conditions

Before the consideration of the heterogeneous nature of the stone, the simulation with homogeneous stone is performed by using a set of material parameters given in table 1.

	Parameter	Tuffeau stone	Mortar
Mechanical parameters	Young's modulus (E [MPa])	1953	1604
	Poisson's coefficient (ν [-])	0.19	0.2
	Mass density (ρ [$\text{kg}\cdot\text{m}^{-3}$])	1300	1240
Hydraulic parameters	Intrinsic permeability (k_{int} [m^2])	1×10^{-13}	0.2×10^{-13}
	Porosity (f [%])	42	50
Thermal parameters	Thermal conductivity (λ [$\text{W}\cdot\text{m}^{-1}\cdot\text{K}^{-1}$])	0.56	0.56
	Heat capacity (C_p [$\text{J}\cdot\text{kg}^{-1}\cdot\text{K}^{-1}$])	830	830
Coupling thermo-hydro-mechanical	Biot's coefficient (b [-])	0.5	0.5
	Thermal expansion coefficient (α [K^{-1}])	6.0×10^{-6}	12×10^{-6} (*)
	Isothermal sorption curve (eq. [3])		

parameters	Pr [MPa] n [-]	0.013 1.37	0.013 (*) 1.37
------------	-----------------------	---------------	-------------------

Table 1. Material parameters for tuffeau stone and mortar

In order to taken into account the spatial variability of the stone, several realizations of normal distribution for three parameters (Young’s modulus, thermal expansion parameter and intrinsic permeability) are performed. Histograms showing the parameter distribution are presented in Figure 2.

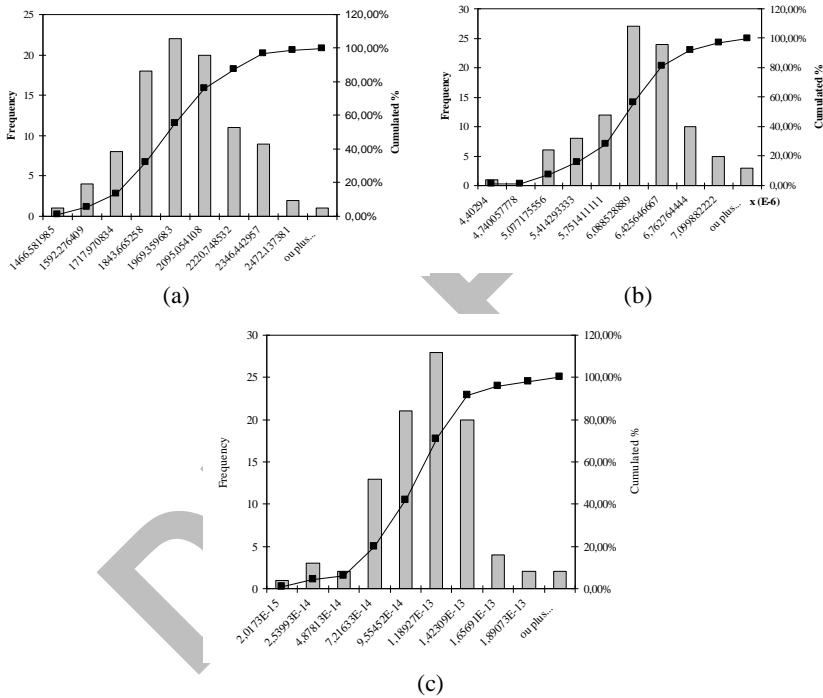


Figure 2. Histograms of normal distribution of (a) Young’s Modulus (b) thermal Expansion coefficient and (c) Permeability.

The mean values of distributions coincide with those of experimental measured properties: for Young’s Modulus the mean value is 1953 MPa, while for the permeability it is 10^{-13} m^2 and for thermal expansion coefficient $6 \cdot 10^{-6} \text{ K}^{-1}$.

To effectively integrate a spatially heterogeneous material in the modeling, the values of the three normally distributions are affected on the zone representing the tuffeau stone block (Figure 1) in random way on the mesh. An example of the contour map of properties distribution is given in Figure 3 for Young’s modulus and thermal expansion coefficient. Similar contours are obtained for permeability. With the aim of comparing the effect of the heterogeneity several simulations were performed affecting

as random distribution either one, two or the three properties. Note that in the case of more than one random variables these spatial distribution are supposed uncorrelated.

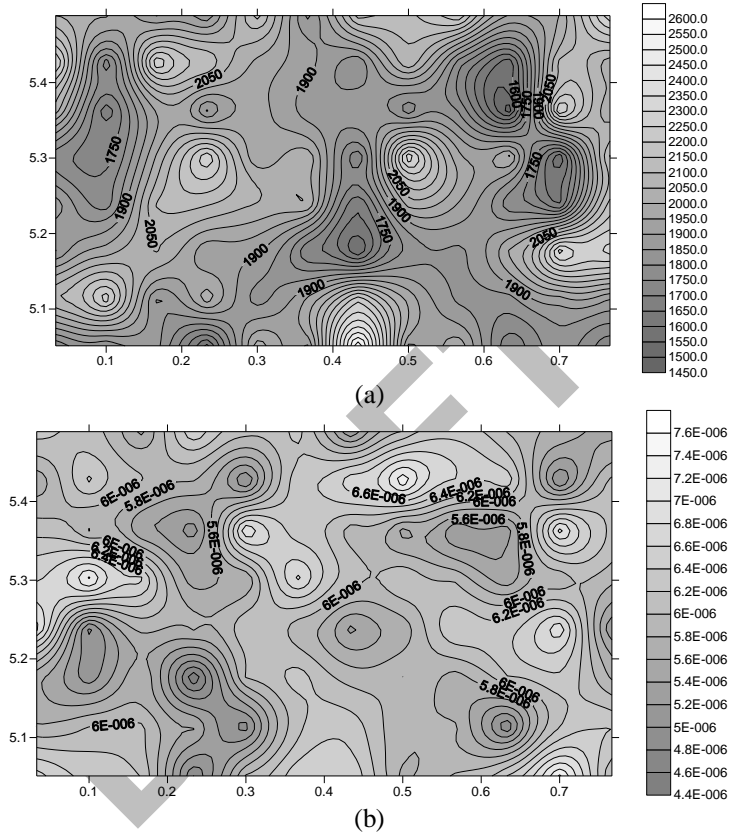


Figure 3. Random distributions of the stone properties affected at the stone mesh, (a) Young's modulus (b) thermal expansion coefficient

3. Results and discussions

The simulations were performed using Code_Aster (EDF) finite element tool taking into account the variations of temperature and humidity for 1 year. The effective stresses for 30 and 366 days at each node of the stone block are calculated. Then, the normalized variance is estimated using the following expression:

$$\psi = \frac{\Delta\sigma - \Delta\sigma_m}{\Delta\sigma_m} \quad \text{with} \quad \begin{cases} \Delta\sigma = \sigma_{\text{spatial variability}} - \sigma_{\text{homogeneous}} \\ \Delta\sigma_m \text{ mean value of } \Delta\sigma \end{cases} \quad [10]$$

According to x axes and y axes the contour maps of this normalized variance are carried out by using geostatistical capabilities of Surfer code. The Figure 4 represents the contour maps of stress variance in the case of Young Modulus heterogeneity. As a

general observation we note that the fluctuation of stresses is amplified because of the spatial variability of the Young's modulus and the variation of temperature and humidity. On the indoor surface the variance is lower in spite of the spatial variability of the mechanical parameter.

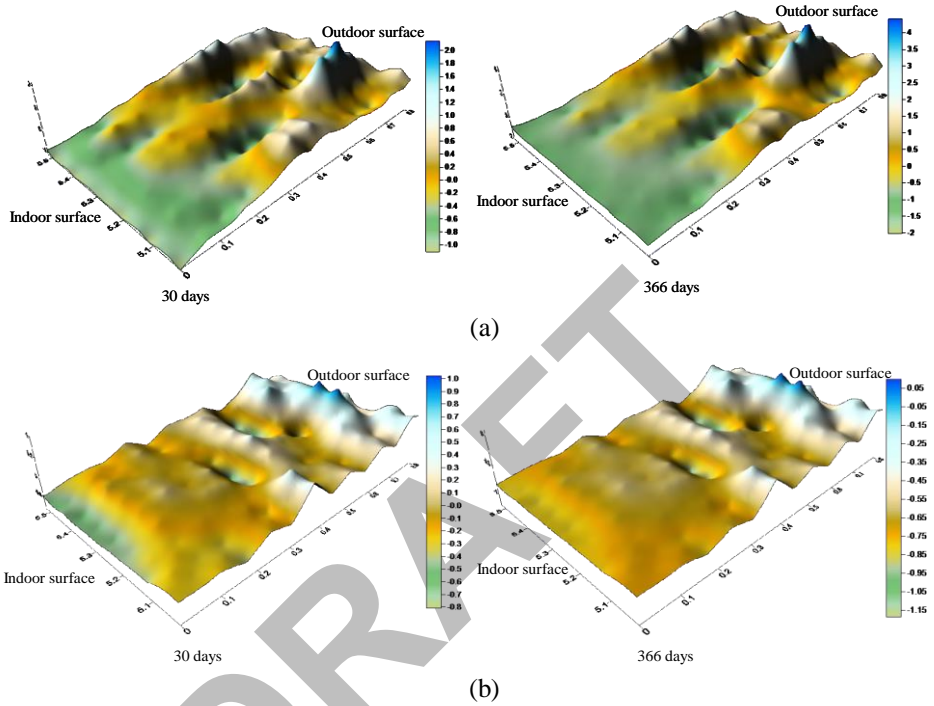


Figure 4. Contour maps of the normalized variance of stresses between the homogeneous and heterogeneous at 30 days and 366 days with normally distributed young's Modulus, (a) according to x axes (b) according to y axes.

One can speculate that the damage due to variation of climate conditions is amplified by the heterogeneous nature of the stone. On Figure 5 the contour maps represented corresponds in the case with thermal expansion coefficient and permeability parameter. In spite the random distribution, the gradient increase towards the outdoor surface with a small vertical fluctuation.

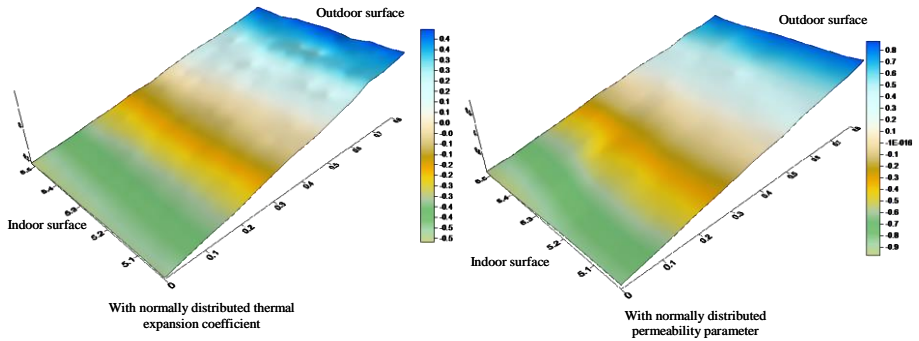


Figure 5. Contour maps of the normalized variance of stresses according to y axes at 366 days with the distribution of thermal and hydraulic parameter.

The Figure 6 shows the effect of the three spatial properties in same time. The points with a maximal variance are different and the gradient is higher than the case of distributed each parameter only.

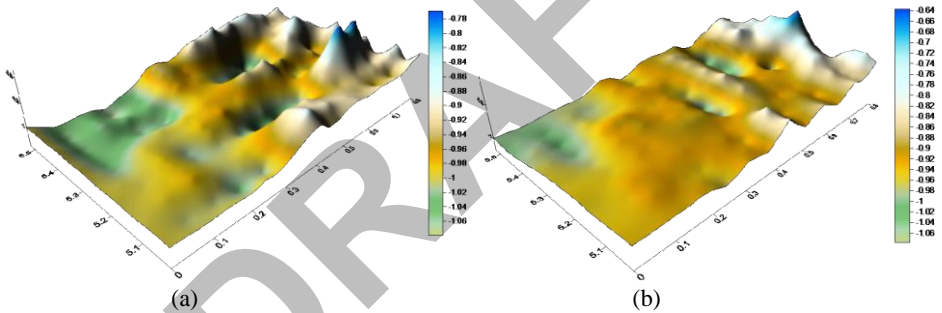


Figure 6. Contour maps of normalized variance between homogeneous case and heterogeneous case with considering the three normally distributed parameter (a) x axes (b) y axes.

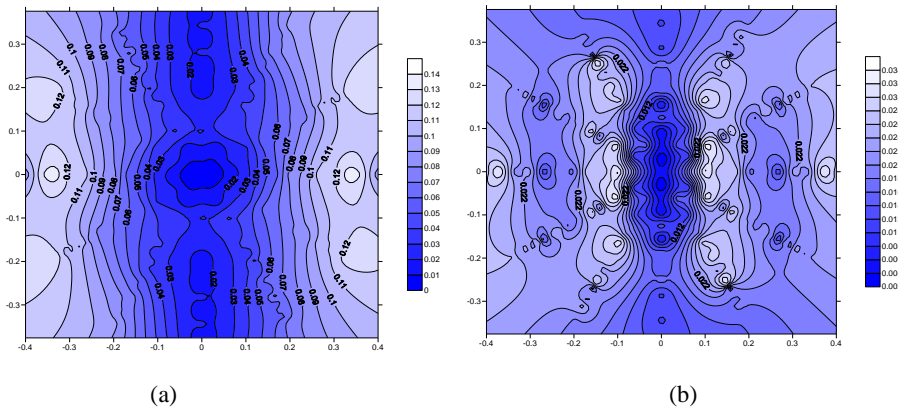


Figure 7. Contour maps of normalized variance between homogeneous case and heterogeneous case with considering the three normally distributed parameter (a) x axes (b) y axes.

On the Figure 7 are illustrated the variomap by using a directional semi-variogram (Yupeng 2011) on the effective stress in the case of normally distributed young modulus.

This variogram map shows that the gradient is very important between two close points than distant points. The difference of contour position is small but suggests that the effect of random distribution on interpolated predictions is greater.

4. Conclusions

An original modeling of a building stones behaviour is presented, combining the thermo-hydronechanical and geostatistical analysis. The results have shown that the spatial variability of the stone properties has an increasing effect on the fluctuation of stresses due to climate variations. The effect of random distribution of mechanical parameter is greater than the thermal and hydraulic ones. The study highlights the combining factors to initiate and evolve the deterioration of the stone buildings. Inspired by these results, the fatigue model taking into account the cyclic variation of climatic conditions and spatial variability will be the immediate continuity of this work.

References

- Beck K., 2006. Etude des propriétés hydriques et des mécanismes d'altération de pierres calcaires à forte porosité, Ph. D dissertation (in French).
- Belayachi, N., Hoxha, D., Do, D., P., 2012. 'thermo-hydro-mechanical behaviour of tuffeau stone masonry,' *European Journal of environmental and civil engineering*, 1-14.
- Castellanza, R., Nova, R., 2004. 'Oedometric Tests on artificially Weathered Carbonatic Soft Rocks', *Journal of Geotechnical and Geoenvironmental Engineering*, ASCE **130**: 728-739.
- Coussy O., 1995. *Mechanics of Porous Continua*. New York: Wiley Ltd.
- K. T. Chau, K. T., Shao, J. F., 2006. 'Subcritical crack growth of edge and center cracks in façade rock panels subject to periodic surface temperature variations', *International Journal of Solids and Structures*, **43**:807-827.
- Chavant C., 2009. 'Modèles de comportement THHM', *Documentation du Code_Aster* R7.01.11 www.code-aster.org. (in French)
- Karoglou M., Moropoulou A., Krokida M.K., Maroulis Z. B., 2007. 'A powerful simulator for moisture transfer in buildings', *Building and Environment*, **42**(2007): 902-912.

- Iwashita, F., Monteiro, R. C., Landim P. M. B., 2005. 'An alternative method for calculating variogram surfaces using polar coordinates', *Computers & geosciences*, **31**:801-803.
- Lopez, D. L., Smith, L., 1996. 'Fluid flow in fault zones: influence of hydraulic anisotropy and heterogeneity on the fluid and heat transfer regime', *Water resources research* **32**:3227-3235.
- Moropoulou, A., Labropoulos, K., Konstanti, A., Roumpopoulos, K., Bakolas, A., Michailidis, P., 2006. 'Susceptibility of building stones to environmental loads: evaluation, performance, repair strategies', In *Fracture and Failure of Natural Building stones*, S. K. Kourkoulis, (Ed.) 291-297.
- Nicholson, D., T., Nicholson, F., H., 2000. 'Physical deterioration of sedimentary rocks subjected to experimental freeze-thaw weathering', *Earth Surface Processes and Landforms*, **25**:1295-1307.
- Rodriguez-Navarro, C., Doehne, E., 1999. 'Salt weathering: influence of evaporation rate supersaturation and crystallization pattern', *Earth Surface Processes and Landforms* **24**:191-209.
- Schulz, S. E., Evans, J. P., 2000. 'Mesoscopic structure of the punchbowl fault, southern California and the geologic and geophysical structure of active strike-slip faults', *Journal of structural geology*, **22**:913-930.
- Warke, P., A., McKinley, J., Smith, B., J., 2006. 'Weathering of building stone: approaches to assessment, prediction and modelling', *Fracture and Failure of Natural Building stones*, S. K. Kourkoulis, (Ed.) 313-327.
- Yupeng, L., Miguel, C., 2011. 'A flexible lag definition for experimental variogram calculation', *Mining science and technology* (China), **21**:207-211.